ELSEVIER

Chemical Engineering Journal 69 (1998) 119–126

Chemical Engineering Journal

Mathematical modeling of monolith reactors for photocatalytic oxidation of air contaminants

Cristiano Nicolella *, Mauro Rovatti

Istituto di Ingegneria Chimica e Processo, Università degli Studi di Genova, Genova, Italy

Received 16 June 1997; revised 12 November 1997; accepted 1 December 1997

Abstract

A distributed parameter model for photocatalytic oxidation of air contaminants in monolith reactors is presented. Heat and mass balance equations for monolith structure are combined with a model of irradiation from a light source and a kinetic model for photon adsorption and chemical reaction to describe the processes of heat, mass and photon transfer within the system and the heterogeneous chemistry at the catalyst surface. The model accounts for interaction between light and matter at the catalyst surface, convective and interphase gas–solid heat and mass transfer, reaction at the catalyst surface and heat conduction within the solid structure. Together with detailed axial profile of temperature and conversion in the gas phase and at the catalyst surface under different operating conditions (inlet gas temperature, composition and flow rate, light source power, monolith geometry), the model provides the distribution of photon flux along the channels and allows the discrimination between thermal and pure photonic effect on the overall rate of conversion.

Keywords: Model; Photocatalysis; Monolith reactor

1. Introduction

Heterogeneous photocatalysis is an innovative and promising approach for rapid, efficient destruction of environmental pollutants that have been proven difficult or expensive to treat using established remediation methods, such as condensation, adsorption and thermal oxidation. In this process, a semiconductor, usually the anatase phase of titanium dioxide, acts as catalytic support for a chemical reaction using light as source of solid excitation.

Although recently, there are a significant number of experiences available in literature which have demonstrated that gas–solid photocatalysis may destroy a wide variety of air contaminants at low temperatures, including acetone [1], toluene and formaldehyde [2], benzene [3], ethanol [4], trichloroethylene [5]. The main advantages claimed for the process include [6]: mild operating conditions (ambient temperature and pressure), safe and available materials, molecular oxygen as oxidant and safe major products.

Glass-plate [2], packed-bed [7], fluidized-bed [8] and monolith [1] reactors have been proposed to absorb light on catalytic supports. Monolithic catalysts have been shown to be very suitable for gas contaminants treatment and are widely used in automotive emission control systems. The advantages of monolithic catalysts are mainly due to their large external surface and low pressure drop. In the case of photoreactor, the geometry of the monoliths is especially appropriate to be coupled with photon absorption because they permit an increase in the lighted area and can be used to volumetrically absorb radiant energy in order to promote heterogeneous chemistry on the catalytic surface with the fluid phase reactant species.

Various aspects of the modeling of monolithic reactors have been published and mono- and multidimensional models have been described and solved [9–20].

In this work, the main concerns of the mathematical modeling of monoliths have extended to the modeling of a reactor for the photocatalytic destruction of air contaminants, the attention being particularly focused on the effect of light adsorption on the heat and mass balance within the reactor and on the overall reaction kinetics.

2. Model

2.1. Assumptions

This study presents the modeling of the physical and chemical processes involved in the photocatalytic oxidation of a

* Corresponding author. Department of Chemical Engineering, Imperial College, Prince Consort Road, London SW7 2BY, UK. Tel.: +44-171-5895111 ext. 55642; fax: +44-171-5945604; e-mail: c.nicolella@ic.ac.uk

1385-8947/98/$19.00
PII S1385-8947(97)00118-6

volatile organic compound (VOC) in a monolith reactor. The considered system incorporates a honeycomb monolith with catalyst particles coated on the surface. The reactor configuration provides illumination of the monolith channels from a lamp located outside the system.

The monolith is composed by a large number of parallel channels whose conditions are supposed to be identical when assuming global adiabacity and uniform distribution of variables at the monolith inlet. Under these hypothesis the simulation of the whole monolith reduces to the analysis of a single channel [18].

To construct a model of physical and chemical processes involved in the photocatalytic oxidation of air contaminants in monolith reactor the following mechanisms are considered: (1) interaction between light and matter at the catalyst surface; (2) adsorption and reaction of reactants on the catalyst surface; (3) convective heat and mass transfer in the gas-phase; (4) interphase heat and mass transfer between the flowing gas and the solid structure; (5) longitudinal heat conduction within the solid structure.

It is assumed that the gas-phase temperature, composition and velocity are uniform across the monolith cross-section. The rate of heat and mass transfer is assumed proportional to the difference between the gas and solid temperature and concentration; the proportionality factors are heat and mass transfer coefficients. The following additional hypothesis are adopted:

- steady state conditions;
- uniform pressure along the monolith channels;
- negligible axial diffusion;
- negligible conduction in the gas phase;
- no reaction in the gas phase.

2.2. Equations

The assumptions adopted for the model result in the following set of equations. (a) Continuity equation:

$$\frac{\mathrm{d}(\rho_g v_g)}{\mathrm{d}x}=0 \tag{1}$$

(b) Equation of state for ideal gas:

$$\rho_g=\frac{M_g P}{RT_g} \tag{2}$$

(c) Enthalpy balance in the gas-phase:

$$S\frac{\mathrm{d}(v_g\rho_g C_{pg}T_g)}{\mathrm{d}x}-\sigma k_h(T_s-T_g)=0 \tag{3}$$

(d) Enthalpy balance at the catalyst surface:

$$S_s\lambda_s\frac{\mathrm{d}^2T_s}{\mathrm{d}x^2}-\sigma k_h(T_s-T_g)+\sigma(-H)k_q+\sigma Q_r=0 \tag{4}$$

(e) Contaminant mass balance in the gas phase:

$$S\frac{\mathrm{d}(v_g C_g)}{\mathrm{d}x}+\sigma k_c(C_g-C_s)=0 \tag{5}$$

(f) Contaminant mass balance at the catalyst surface

$$k_c(C_g-C_s)-k_q=0 \tag{6}$$

The boundary conditions are:

$$\begin{aligned} & & C_g&=C_{gi} \\ x=0 \quad &\rightarrow & T_g&=T_{gi} \\ & & -\lambda_s\frac{\mathrm{d}T_s}{\mathrm{d}x}&=\alpha f h\nu N_A \\ x=L \quad &\rightarrow & \frac{\mathrm{d}T_s}{\mathrm{d}x}&=0 \end{aligned} \tag{7}$$

2.3. Kinetic modeling

The mechanisms involved in the processes of excited states in photocatalysis are fully described in Ref. [21].

A catalyst molecule can be promoted from the ground state to an excited state by the adsorption of a quantum of light. The necessary condition is that the photon energy, $h\nu$, matches the energy gap between the ground and the excited state. This energy gap, for low-energy states of common inorganic molecules, corresponds to light in the visible and near-ultraviolet region.

The excited molecules can return to the ground state by following three different pathways: (1) radiative deactivation with emission of a quantum of light, (2) radiationless deactivation with isoenergetic conversion of the energy of the upper state into vibrational energy of the lower state and vibrational relaxation of the lower state, and (3) chemical reaction with the quenching of the activated site.

The three processes have their individual rates and compete with each other for the deactivation of any activated catalyst site; a quantum yield is defined for each process as the ratio between the number of molecules undergoing the process per unit of time and the number of photons adsorbed on the catalyst surface per unit of time.

The overall mechanism of light adsorption, catalyst photoactivation, catalyst deactivation, energy transfer and chemical reaction is schematically represented in Fig. 1.

The number of catalyst sites activated by light is supposed to be equal to the number of photons adsorbed on the catalyst surface, which can be calculated from the photon flux (f) on the surface through a light adsorption coefficient (α).

It is assumed that the photocatalytic oxidation of air contaminants develops through two consecutive steps: (1) energy transfer from an excited catalyst site to a contaminant molecule adsorbed on the catalyst surface; (2) chemical reaction of the excited VOC and the oxygen at the catalyst surface.

The rate of energy transfer is:

$$k_e=\alpha f-k_r-k_{nr}=\eta_e\alpha f \tag{8}$$

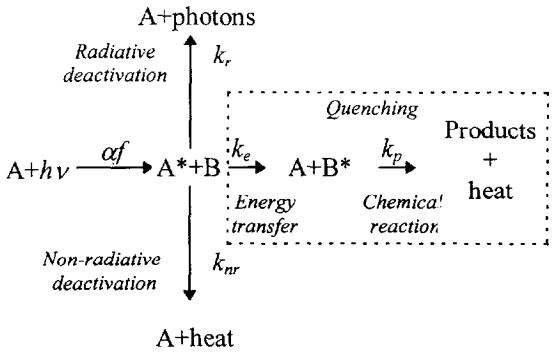

Fig. 1. Processes involved in photocatalytic reactions. A: catalyst; A*: excited catalyst; B: reactant; B*: excited reactant; α: light absorption coefficient; f: photon flux; k_r: rate of radiative deactivation; k_{nr}: rate of nonradiative deactivation; k_e: rate of energy transfer; k_p: rate of chemical reaction.

if $\eta_e \alpha f$, where η_e is the quantum yield of the process of energy transfer, is lower than the rate of VOC mass transfer from the gas phase to the catalyst surface. Otherwise, k_e must balance the VOC mass transfer rate. In the first case, the excited catalyst sites in excess return to the ground state either through a radiative deactivation or a nonradiative deactivation.

As the oxygen concentration at the catalyst surface is supposed to be much higher than the VOC concentration in the system under study, the rate of the chemical reaction (k_p) is regarded as first order in the VOC concentration at the catalyst surface. The effectiveness factor η (calculated according to Ref. [22]) is introduced to characterize the diffusion of reactants and products within the catalyst pores. k_p is expressed by:

$$k_p = \eta A_p e^{-E_p/RT_s} C_s \delta. \tag{9}$$

For the estimation of the overall rate of quenching (k_q), the rate of energy transfer, k_e, and the rate of chemical reaction, k_p are compared and two limiting cases are considered (see Fig. 1).

$$\begin{aligned} &k_p \gg k_e \Rightarrow k_q = k_e \\ &k_p \ll k_e \Rightarrow k_q = k_p. \end{aligned} \tag{10}$$

2.4. Model parameters and physical properties

2.4.1. Heat transfer by radiation

The heat transferred at the catalyst surface from the light source is the sum of three contributions: (1) overplus of photon energy compared to energy gap between the ground and excited state of the catalyst sites; (2) heat dissipated by the vibrational relaxation of the catalyst activated sites during the non-radiative deactivation; (3) heat dissipated by the vibrational relaxation of the excited reactant molecules which do not participate in the reaction.

Therefore, the heat transfer due to the radiation of light is:

$$Q_r = \alpha f N_A h\nu - k_q N_A E_{gap}. \tag{11}$$

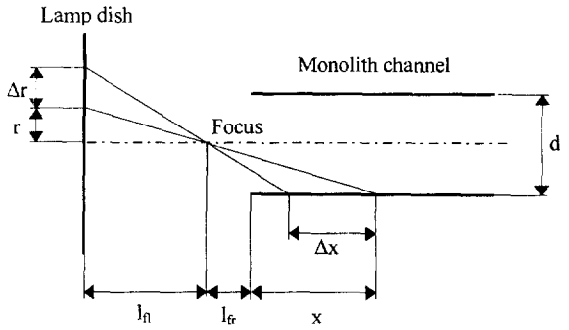

Fig. 2. Schematic representation of the lamp and monolithic reactor. r: lamp radial coordinate; Δr: lamp annulus width; x: channel axial coordinate; Δx: channel element width; l_{fl}: distance between focus and lamp; l_{fr} distance between focus and reactor; d: channel diameter.

2.4.2. Photon flux

Light represents the energy source for the activation of the catalyst sites. In the considered system, the monolith channels are supposed to be irradiated from outside the reactor by a near-UV lamp.

The following assumptions are made for the description of the irradiation:

- the lamp is a circular dish;
- the rays are concentrated in a focus;
- the light is monochromatic;
- reflection and scattering are negligible;
- the monolith channel is placed axially with the lamp.

The system constituted by the lamp and monolith is schematically represented in Fig. 2. In the present description each irradiated point of the monolith surface is associated to a point of the lamp. Easy geometrical considerations allow to calculate the width (Δr) and position (r) of an annulus on the lamp surface as a function of the width (Δx) and position (x) of the correspondent element on the catalyst surface and to define the photon flux (f) in each point of the channel surface as a function of the axial coordinate:

$$r = \frac{dl_{fl}}{2(x + l_{fr})} \tag{12}$$

$$\Delta r = \frac{dl_{fl}}{2(x + l_{fr})^2} \Delta x. \tag{13}$$

After defining a function of flux distribution:

$$\mathrm{FDF} = \frac{2\pi f(x) g(x)}{\sigma} \tag{14}$$

the photon flux on the channel wall can be calculated through:

$$f = \frac{2\pi r W \Delta r}{N_A h\nu \sigma \Delta x} = \frac{W}{N_A h\nu} \mathrm{FDF}. \tag{15}$$

2.4.3. Heat and mass transfer coefficients

The heat and mass transfer coefficient are evaluated from the relationships proposed by Refs. [10,11].

$$\mathrm{Nu}=0.571\left(\mathrm{Re}\frac{d}{L}\right)^{2/3}$$

$$\mathrm{Sh}=0.705\left(\mathrm{Re}\frac{d}{L}\right)^{0.43}\mathrm{Sc}^{0.56} \qquad (16)$$

2.4.4. Catalyst and fluid properties

The physical properties of the solid matrix considered in the solution of the model are referred to those of titanium dioxide supported on sepiolite, since TiO_2 is usually employed in the photocatalytic treatment of air streams containing VOCs.

The estimation of the active catalyst volume was derived from Ref. [1].

The fluid flowing in the monolith channel consists of a mixture of air and a contaminant. Since the reactor is designed to treat air streams at low pollutant concentration, the physical properties of the gas-phase are referred to those of the air. The values of these properties and, where significant, the dependence on the fluid temperature are calculated according to the relationships reported in Ref. [22].

2.5. Integration

On using the following parameters:

$$y=\frac{C_{gi}-C_g}{C_{gi}} \quad J_D=\frac{\sigma L k_c}{S v_{gi}} \quad f^*=\frac{\sigma L W}{S v_{gi} C_g N_A h \nu}$$

$$w=\frac{C_{gi}-C_s}{C_{gi}} \quad J_H=\frac{\sigma k_h L}{S v_{gi}\rho_{gi} C_p} \quad B=\frac{[(-\Delta H)-E_{gap}N_A]C_{gi}\gamma}{\rho_{gi}C_p T_{gi}}$$

$$t=\frac{E}{RT_{gi}^2}(T_g-T_{gi}) \quad \gamma=\frac{E_p}{RT_{gi}} \quad Q_r^*=\frac{N_A h\nu C_{gi}\gamma}{\rho_{gi}C_p T_{gi}}$$

$$u=\frac{E}{RT_{gi}^2}(T_s-T_{gi}) \quad \mathrm{Da}=\frac{L\delta\sigma A_p e^{-\gamma}}{S v_{gi}} \quad k_e^*=\frac{\eta_e \alpha f}{\mathrm{Da}}\mathrm{FDF}$$

$$z=\frac{x}{L} \quad \mathrm{Pe}=\frac{SLv_{gi}\rho_{gi}C_p}{S_s\lambda_s} \quad k_p^*=\Phi\exp\left(\frac{u}{u/\gamma+1}\right)(1-w)\frac{\delta}{\delta_a} \qquad (17)$$

the governing transport equations (Eqs. (1)–(6)) along with the boundary conditions (Eq. (7)) and the expressions for the chemical reaction rate and energy transfer rate (Eqs. (8)–(10)) may be rendered dimensionless.

$$\frac{\mathrm{d}\left[\left(\frac{t}{\gamma}+1\right)y\right]}{\mathrm{d}z}+J_D(y-w)=0 \qquad (18)$$

$$\frac{\mathrm{d}u}{\mathrm{d}z}+J_H(t-u)=0 \qquad (19)$$

$$J_D(y-w)+\mathrm{Da}k_q^*=0 \qquad (20)$$

$$\frac{1}{\mathrm{Pe}}\frac{\mathrm{d}^2u}{\mathrm{d}z^2}-J_H(u-t)+B\mathrm{Da}k_q^*+Q_r^* f^*\mathrm{FDF} \qquad (21)$$

$$z=1;\ y=1;\ t=1;\ \frac{\mathrm{d}u}{\mathrm{d}z}=-\mathrm{Pe}Q_r^* f^*\mathrm{FDF}\frac{S_s}{\sigma L}$$

$$z=1:\frac{\mathrm{d}u}{\mathrm{d}z}=0 \qquad (22)$$

The set of model equations constitutes a nonlinear boundary-value problem. The solution of the differential equations is obtained through a finite difference representation of the derivatives [23]. The resulting nonlinear equations are solved by means of the Newton–Rapheson method.

3. Results and discussion

Some of the parameters introduced to describe the photooxidation of air contaminants in monoliths reactors are those usually employed to describe heterogeneous catalysis (Pe, Da, J_D, J_H). The influence of these parameters on the photocatalytic process is qualitatively similar to the influence that the same parameters have in pure thermal catalysis (without any effect of light). As an example, Fig. 3 reports the conversion profile along the monolith channel as a function of the Damkohler number, while Fig. 4 reproduces the calculated wall temperature along the channel as a function of the Peclet number.

Due to the low adiabatic temperature rise and the high Peclet number which typically characterize monolith reactors for photoassisted oxidation of air contaminants the processes are expected to occur in the region of unicity of steady states [10,11]. In fact photocatalytic reactors are normally used for the oxidation of low concentration contaminants in gaseous streams; under these conditions, the adiabatic temperature rise in a monolith channel is actually low. Moreover the active phase for photocatalyzed reactions is generally supported on non-metallic materials characterized by low thermal conductivity.

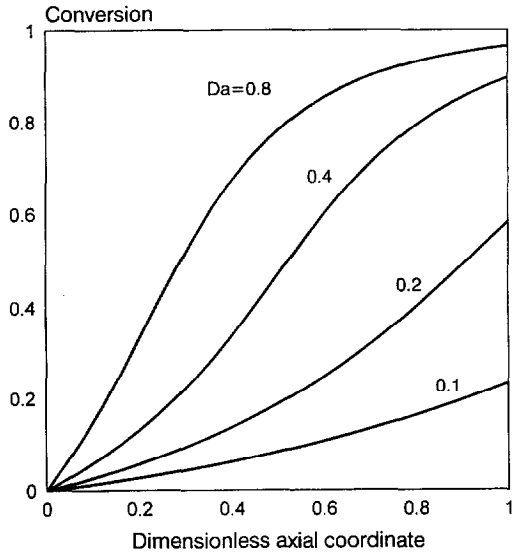

Fig. 3. Effect of Damkohler number on the shape of conversion profile ($B=3.6$, $Q_r^*=0.3$, $f^*=1363$, $J_D=7$, $J_H=12$, Pe = 102, $\gamma=17.3$).

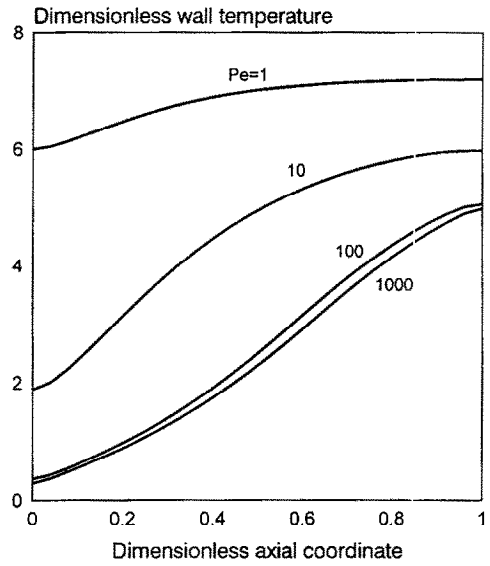

Fig. 4. Effect of Peclet number on the shape of wall temperature profile ($B=3.6$, $Q_r^*=0.3$, Da $=0.3$, $f^*=1363$, $J_D=7$, $J_H=12$, $\gamma=17.3$).

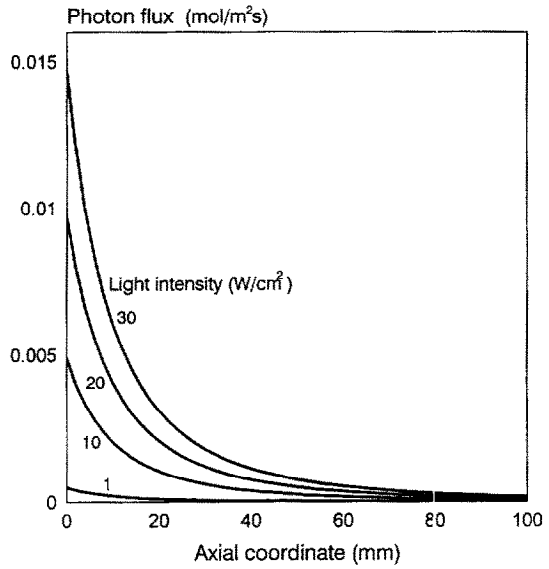

Fig. 5. Photon flux profile along the channel for different values of light intensity.

The innovative aspect of the present work could be related to the capability of describing the interaction between light and matter at the catalyst surface in the considered system.

Photons are in general the most expensive component of photocatalytic reactors and criteria for their effective use are very important in the design and operation of these systems. The photon flux on the channel wall as calculated through Eqs. (12)–(15) is depicted in Fig. 5 for different values of light intensity. The shape of the curves in Fig. 5 does not depend only on light intensity but also on the mutual position of light source, focus and reactor. It is evident from Fig. 5 that only the first part of the reactor is fully irradiated and the intensity of the incident photon flux decreases rapidly along the channel length. This implies that only a limited part of a monolith can be effectively photoactivated, this being an additional constraint in the design of the system.

Fig. 6 reports the model estimation of the rate of energy transfer (k_e) and chemical reaction (k_p) corresponding to different values of the Damkohler number and dimensionless photon flux. Depending on these parameters the step controlling the overall process rate shifts from the energy transfer (Fig. 6a) to the chemical reaction (Fig. 6c). From the point of view of process optimization, the most attractive situation is that represented in Fig. 6a, where the transfer of photons is the controlling step throughout the channel length: in this case a photonic regime can be defined where all the incident photons are used to activate the sites on the catalytic surface. If the controlling step is the chemical reaction, only a fraction of the photon flux is directly involved in the reaction process at the monolith wall, the remaining part being used to heat up the surface. In this case it is not possible to distinguish between pure photonic effect and pure thermal effect and we can therefore define a regime of thermal operation. Under the conditions typical of photonic regime (low f^*/Da ratio) the overall reaction rate does not depend directly on the wall temperature, whilst it does under the conditions of thermal regime (high f^*/Da ratio).

If the Damkohler number is relatively high, the portion of the reactor characterized by photonic regime corresponds to

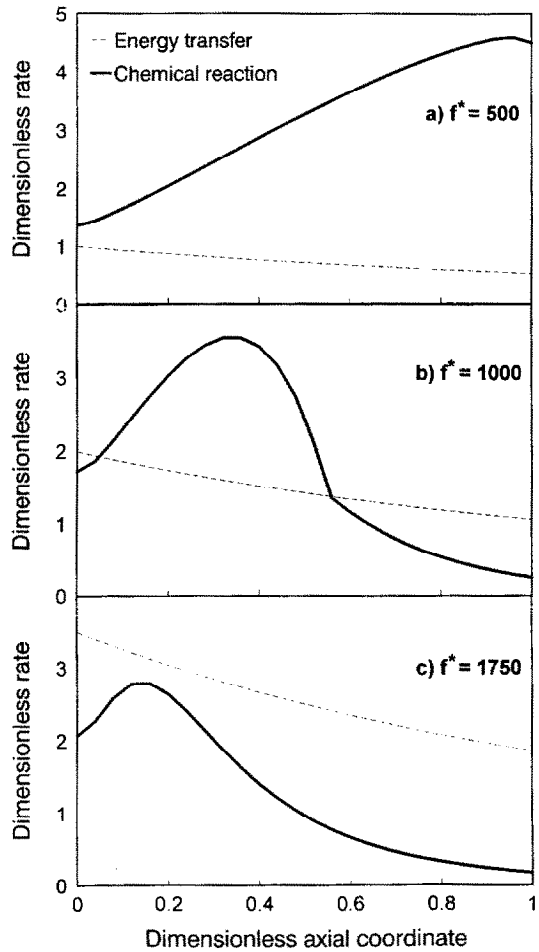

Fig. 6. Profiles of energy transfer and chemical reaction rate for different values of the dimensionless photon flux ($B=3.6$, $Q_r^*=0.3$, Da $=1$, $J_D=7$, $J_h=12$, Pe $=102$, $\gamma=17.3$). (a) $f^*=500$; (b) $f^*=1000$; (c) $f^*=1750$.

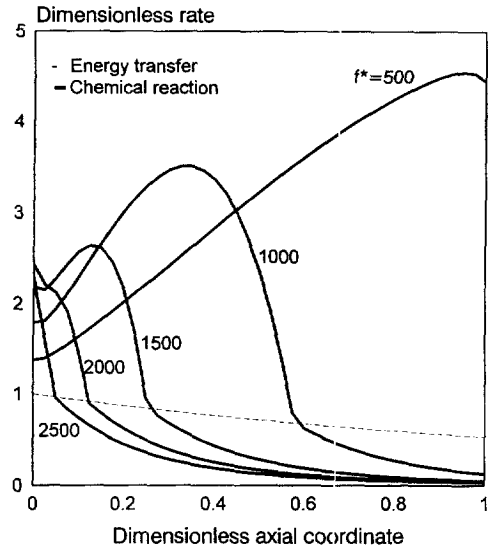

Fig. 7. Effect of Damkohler number and photon flux on the profiles of energy transfer and chemical reaction rate along the channel ($B=3.6$, $Q_r^*=0.3$, $f^*/\mathrm{Da}=500$, $J_D=7$, $J_H=12$, $\mathrm{Pe}=102$, $\gamma=17.3$).

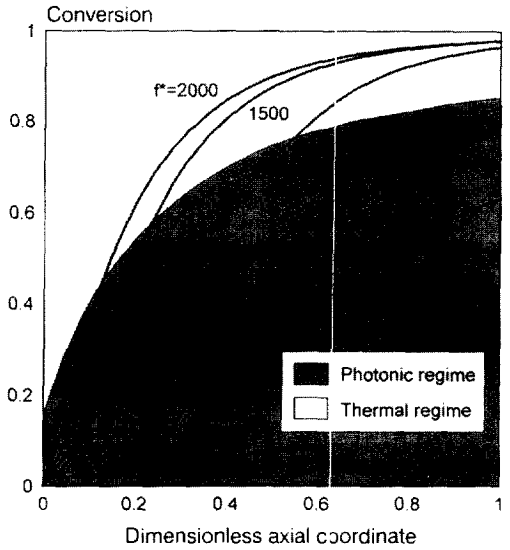

Fig. 8. Effect of photon flux on the conversion profiles along the channel ($B=3.6$, $Q_r^*=0.3$, $\mathrm{Da}=0.3$, $J_D=7$, $J_H=12$, $\mathrm{Pe}=102$, $\gamma=17.3$).

the initial part of the channel, where the photon flux is highest. This situation should be seen as optimal for the best utilization of photons.

The transition from photonic to thermal regime is influenced by many operating variables such as photon flux, wall temperature, residence time of the gas phase, and by the characteristics of the reactants. The effect of these parameters can be included in the Damkohler number and photon flux and it is represented in Fig. 7, which reports the position of the transition between photo-and thermal effect for different values of Da as a function of the dimensionless photon flux. The position of the discontinuity in k_p, corresponding to the transition from photonic to thermal regime, moves towards the entrance of the reactor when Da increases.

The influence of the radiation on the reactor performance is plotted in Fig. 8 which reports the conversion profiles along

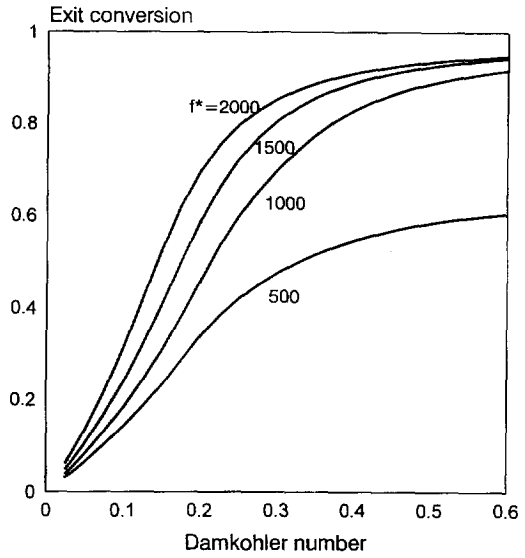

Fig. 9. Effect of photon flux and Damkohler number on the exit conversion ($B=3.6$, $Q_r^*=0.3$, $J_D=7$, $J_H=12$, $\mathrm{Pe}=102$, $\gamma=17.3$).

the channel as a function of the dimensionless photon flux. For high values of f^* (thermal regime) the reaction zone moves towards the monolithic module entrance. In Fig. 8, the cross hatched area delimitates the region within the reactor characterized by photonic regime. At high photon flux the exit conversion is high but most part of the reactor works under thermal effect. For the set of parameters used to calculate the model solution reported in Fig. 8 the best conversion under pure photonic effect is about 0.86, reached at $f^*=750$.

The combined effect of photon flux and chemical reaction rate is represented in Fig. 9. The exit conversion is plotted as a function of the Damkohler number for different values of the dimensionless photon flux. Fig. 9 does not allow to discriminate between thermal and photonic effect and should be combined to Fig. 8 to evaluate the role of photoassisted catalysis in each particular situation.

4. Conclusions

Physical and chemical processes involved in the photocatalytic oxidation of air contaminants in monolith reactors were analyzed in terms of heat and mass balance equations. The innovative aspect of the modeling is the description of the interaction between light and matter at the catalyst surface which allows the rate of chemical reaction and energy transfer to be computed. Depending on the rate of these two processes a photonic regime and a thermal regime are defined and criteria for the optimal operation of the reactor are given. It is expected that the results of modeling will assist in the design of versatile catalytic systems for the photoassisted oxidation of air contaminants.

5. Nomenclature

A_p	frequency factor	s^{-1}
B	dimensionless adiabatic temperature rise	
C	concentration	mol/m^3
C_p	specific heat	J/(kg K)
d	channel diameter	m
D	diffusion coefficient	m^2/s
E_{gap}	gap energy	J
E_p	activation energy	J/mol
f	photon flux	$mol/(m^2\ s)$
FDF	flux distribution function	
$h=6.63\times10^{-34}$	Plank constant	J/s
H	heat of reaction	J/mol
k_c	mass transfer coefficient	m/s
k_e	energy transfer rate	$mol/(m^2\ s)$
k_h	heat transfer coefficient	$J/(m^2\ s\ K)$
k_{nr}	radiationless deactivation rate	$mol/(m^2\ s)$
k_p	reaction rate	$mol/(m^2\ s)$
k_r	radiative deactivation rate	$mol/(m^2\ s)$
k_q	quenching rate	$mol/(m^2\ s)$
l_{fl}	distance focus-lamp	m
l_{fr}	distance reactor-lamp	m
L	channel length	m
$N_A=6.02\times10^{23}$	Avogadro number	
M	molecular weight	kg/kmol
P	pressure	Pa
Q_r	heat transfer by radiation	$J/(m^2\ s)$
r	lamp radial coordinate	m
$R=8.31$	universal gas constant	J/(mol K)
S	channel void cross-section area	m^2
S_s	channel wall cross-section area	m^2
t	dimensionless gas temperature	
T	temperature	K
u	dimensionless wall temperature	
v	velocity	m/s
w	conversion on catalyst surface	
W	lamp power	W
x	channel axial coordinate	m
y	conversion in gas phase	
z	dimensionless axial coordinate	

Greek letters

α	light adsorption coefficient	
δ	catalyst thickness	m
δ_a	active catalyst thickness	m
Φ	effectiveness factor	
γ	dimensionless activation energy	
η_e	quantum yield of energy transfer	
η_{nr}	quantum yield of non-radiative deactivation	
η_r	quantum yield of radiative deactivation	
λ	thermal conductivity	W/m K
υ	light frequency	s^{-1}
ρ	density	kg/m^3
σ	wet perimeter	m

Dimensionless parameters

Da	Damkohler number (see Eq. (17))
$Nu=(dk_h)/\lambda_g$	Nusselt number
$Re=(\rho_g v d)/\mu_g$	Reynolds number
$Sc=(D\rho_g)/\mu_g$	Schmidt number
$Sh=(dk_c)/D$	Sherwood number

Subscripts

g	gas phase
s	solid phase
i	inlet conditions

Superscript

*	dimensionless

Acknowledgements

Research supported by EU within the Environment and Climate research program (contract no. EV5V-CT94-0558).

References

[1] M.L. Sauer, D.F. Ollis, J. Catal. 149 (1994) 81–91.
[2] T.N. Obee, Environ. Sci. Technol. 30 (1996) 3578–3584.
[3] X. Fu, W.A. Zeltner, M.A. Anderson, Appl. Catal. B 6 (1995) 209–224.
[4] M.R. Nimlos, E.J. Wolfrum, M.L. Brewer, J.A. Fennel, G. Bintner, Environ. Sci. Technol. 30 (1996) 3102–3110.
[5] W.A. Jacoby, M.R. Nimlos, D.M. Blake, R.D. Noble, C.A. Koval, Environ. Sci. Technol. 28 (1994) 1661–1666.
[6] J. Peral, D. Ollis, Heterogeneous photocatalysis for purification, decontamination and deodorization of air, Proceedings of the 6th International Symposium on Solar Thermal Concentrating Technologies, Mojacar, 1992, pp. 1233–1243.
[7] L.A. Dibble, G.B. Raupp, Catal. Lett. 4 (1990) 345–354.
[8] L.A. Dibble, G.B. Raupp, Environ. Sci. Technol. 26 (1992) 492–495.
[9] R.H. Heck, J. Wei, J.R. Katzer, AIChE J. 22 (1976) 477–484.

[10] J. Votruba, J. Sinkule, V. Hlavacek, J. Skrivanek, Chem. Eng. Sci. 30 (1975) 117–123.
[11] J. Votruba, O. Mikus, K. Nguen, V. Hlavacek, J. Skrivanek, Chem. Eng. Sci. 30 (1975) 201.
[12] L.C. Young, B.A. Finlayson, AIChE J. 22 (1976) 331–343.
[13] S. Lee, R. Aris, Chem. Eng. Sci. 32 (1977) 827–837.
[14] J. Sinkule, V. Hlavacek, Chem. Eng. Sci. 33 (1978) 839–845.
[15] K. Zygourakis, R. Aris, Chem. Eng. Sci. 38 (1983) 733–744.
[16] K. Zygourakis, Chem. Eng. Sci. 44 (1989) 2075–2086.
[17] R.E. Hayes, S.T. Kolaczkowski, W.J. Thomas, Comput. Chem. Eng. 16 (1992) 645–657.
[18] G. Groppi, A. Belloli, E. Tronconi, P. Forzatti, AIChE J. 41 (1995) 2250–2260.
[19] G. Groppi, A. Belloli, E. Tronconi, P. Forzatti, Chem. Eng. Sci. 50 (1995) 2705–2715.
[20] R.E. Hayes, S.T. Kolaczkowski, W.J. Thomas, J. Titiloye, Ind. Eng. Chem. Res. 35 (1996) 406–414.
[21] V. Balzani, F. Scandola, Interaction between light and matter, in: N. Serpone, E. Pellizzetti (Eds.), Photocatalysis, Wiley, New York, 1989.
[22] R.H. Perry, D. Green, Chemical Engineers' Handbook, 6th edn., McGraw-Hill, New York, 1984.
[23] B.A. Finlayson, Nonlinear Analysis in Chemical Engineering, McGraw-Hill, New York, 1980.